Hindawi
Journal of Sensors
Volume 2018, Article ID 5419645, 8 pages
https://doi.org/10.1155/2018/5419645

*Research Article*

# Deep Denoising Autoencoding Method for Feature Extraction and Recognition of Vehicle Adhesion Status

**Jing He, Linfan Liu, Changfan Zhang, Kaihui Zhao, Jian Sun, and Peng Li**

*Hunan University of Technology, Zhuzhou 412007, China*

Correspondence should be addressed to Changfan Zhang; zhangchangfan@263.net

Received 28 May 2017; Revised 31 August 2017; Accepted 17 September 2017; Published 16 September 2018

Academic Editor: Jing Xu



Feature extraction and classification for deep learning are studied to recognize the problem of vehicle adhesion status. Data concentration acquired by automobile sensors contains considerable noise. Thus, a sparse autoencoder (stacked denoising autoencoder) is introduced to achieve network weight learning, restore original pure signal data by use of overlapping convergence strategy, and construct multiclassification support vector machine (SVM) for classification. The sensors are adopted in different road environments to acquire data signals and recognize the adhesion status online. Results show that the proposed method can achieve higher accuracies than those of the adhesion status recognition method based on SVM and extreme learning machine.

## 1. Introduction

Research on intelligent vehicles mainly aims to improve the safety and comfort of automobiles [1]. In recent years, sensor technology has developed rapidly [2, 3]. Active safety technology that prevents accidents has developed rapidly with the development of sensor and control technologies; the technology is also called advanced driver assistance system (ADAS), which has become a popular research topic in the field of intelligent vehicle [4]. Timely identification of intelligent vehicle adhesion status can prevent driving wheels from slipping excessively when cars start and accelerate. Adhesion status caused by a complicated road environment is difficult to recognize. The recognition of adhesion status determines the target value of engine output torque. If the torque control target is unsuitable, then the high side drive slips; the traction control system should then brake the high side, and the braking and driving forces counteract, thereby causing car buffeting.

Scholars have conducted extensive research on road surface adhesive recognition. Yoon et al. [5] estimated the adhesion status of a vehicle by use of a magnetic field meter and Global Positioning System (GPS). Erdogan et al. [6] implanted a special sensor inside the tire to estimate the adhesion status of a vehicle. Han et al. [7] predicted the friction coefficient of a vehicle with sensors by use of six degrees of freedom to increase robustness. The equipment used in the abovementioned method is costly, thereby increasing the manufacturing cost. A few scholars have conducted adhesion recognition studies by use of existing sensors. Bevly et al. [8] proposed a method for measuring vehicle state-wheel slip by use of GPS velocity information in conjunction with other sensors. Considering the noise problem in adhesion status recognition, Enisz et al. [9] proposed an algorithm based on a filter to estimate the coefficients of adherent and friction by adopting unscented Kalman. Xu et al. [10] determined the best point-of-slip ratio by proposing an online search method based on an observer. A signal convergence method that combines available signals is proposed to estimate the friction force in [11]. Deep learning originates from the study of neural network, obtains deep feature representation, and solves the noise problem [12]. However, deep learning applied in the recognition of vehicle adhesion status has been unreported.

Stacked denoising autoencoder (SDAE) method regards noise reduction as the criterion of web-based learning. Training can add a different intensity of noise in the input signal. Thus, the encoding process of the method exhibits good

stability and robustness. Zhang et al. [13] indicated that the synthetic minority oversampling technique (SMOTE) causes a noise problem when synthesizing minority oversampling. An improved noise reduction self-encoding (SMOTE combined with SDAE (SMOTE-SDAE)) was thus proposed. Ueda et al. [14] combined SDAE and a filter to recognize the voice of reverberation environments. Li et al. [15] conducted brain electrical signal decoding by SDAE and obtained correct recognition but with incomplete signal. Xia et al. [16] proposed an improved SDAE, recognized acoustic emotion, and obtained a good effect.

In the current study, sparse SDAE is investigated to build a laminated deep network and realize the recognition of vehicle adhesion status. To acquire deep characteristics from data and improve vehicle adhesion status (normal, fault symptoms, minor faults, and serious faults), the differences between them are obtained by use of SDAE, thereby making them suitable for the characteristics of the classifiers. Parametric rectified linear unit (PReLU) is used as the activation function in SDAE to extract high-level and sparse features. Support vector machine (SVM) is used to classify the said characteristics.

The rest of the paper is organized as follows. Section 2 describes the recognition problem of vehicle adhesion status. Section 3 introduces the principle of SDAE. The SVM model is proposed to recognize vehicle adhesion status. Section 4 discusses the simulation experiment. Finally, Section 5 elaborates the conclusions of the study.

## 2. Recognition Problem of Vehicle Adhesion Status

This study focuses on an individual wheel, which is one-fourth of the vehicle model, as shown in Figure 1.

The equations of motion force and friction are expressed as [17]

$$\begin{aligned} M\mathrm{v}_{\omega}' &= -F_N - F_w - f, \\ J\omega' &= R(F_N + F_\omega) - T, \\ \mu &= \frac{F_N}{N}, \end{aligned} \tag{1}$$

where $M$ is the mass of vehicle, $F_N$ is the friction force of vehicle, $F_\omega$ is the resistance of the vehicle wheel, $f$ is the air friction, $T$ is the breaking torque, $J$ is the rotational inertia of vehicle, $R$ is the radius of vehicle, $\omega$ is the angular velocity of vehicle, $\mu$ is the attachment coefficient, and $N$ is the normal force between the vehicle and the ground.

The attachment coefficient possesses a close relationship with the slip rate of vehicle, which can be defined as follows [18]:

$$\lambda = \frac{V - \omega R}{V}, \tag{2}$$

where $V$ is the actual driving speed, $\omega$ is the angular velocity of vehicle, and $R$ is the radius of vehicle.

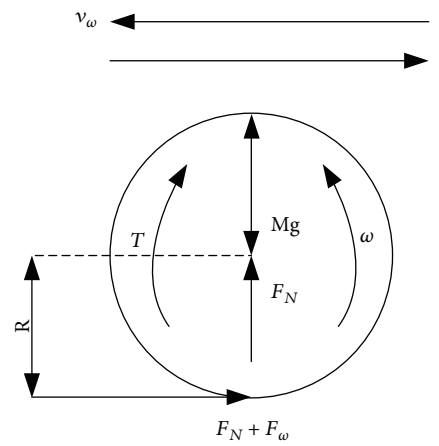


Figure 1: One-fourth of the vehicle model.

The attachment coefficient and slip rate of vehicle present a nonlinear relationship. In Burckhardt's model, the attachment coefficient is described as follows [19]:

$$\mu(\lambda) = \left[c_1\left(1 - \mathrm{e}^{-c_2\lambda}\right) - c_3\lambda\right], \tag{3}$$

where $c_1$, $c_2$, and $c_3$ are constants. Parameter values in different road conditions are shown in Table 1.

Figure 2 shows the relationship curve of the attachment coefficient and slip rate of vehicle. The maximum attachment coefficient $\mu_{\max}$ and the corresponding slip rate $\lambda_{\max}$ exist in every curve. Peak areas on both sides are called stable region and the unsteady area of driving. The SVM for recognizing adhesion status adopts the offline training model. A deep denoising autoencoding method is proposed to explore the information encoded in the state, and the adhesion status is classified into four levels by applying support vector convergence. These statuses are normal, failure symptom, small fault, and major failure. By applying vectors installed in the vehicle, ADAS collects the environment state inside and outside the vehicle in a timely manner to process the recognition, sense, and trace of static and dynamic objects and thus reduce risks that can be detected by the driver and improve the active safety technology [20]. The adhesion state is divided into four categories, thereby providing new ideas for early risk warning of ADAS. When a minor fault is encountered, some control methods can be adopted to adjust the slip rate to the best status.

## 3. Principle of SDAE

*3.1. Denoise Autoencoder (DAE).* An automatic encoder (AE) output can reproduce input, but the effect is not improved when considerable amount of noise exists in the data set. The car running environment is complicated. Oil, rain, snow, mud, and other media influence the identification of the car adhesion state. On the basis of AE, DAE links a certain probability distribution of noise to the input data, performs AE learning to remove the noise, and reconstructs the nondisrupted input. Thus, the characteristics obtained

Table 1: Parameter values in different road conditions.

| Pavement condition | $c_1$ | $c_2$ | $c_3$ |
|---|---|---|---|
| Dry asphalt | 1.2801 | 23.99 | 0.52 |
| Wet asphalt | 0.8570 | 33.822 | 0.347 |
| Dry cement | 1.1973 | 25.168 | 0.5373 |
| Dry cobblestone | 1.3713 | 6.4565 | 0.6691 |
| Wet cobblestone | 0.4004 | 33.7080 | 0.1204 |
| Snow | 0.1946 | 94.129 | 0.0646 |
| Ice | 0.05 | 306.39 | 0.001 |

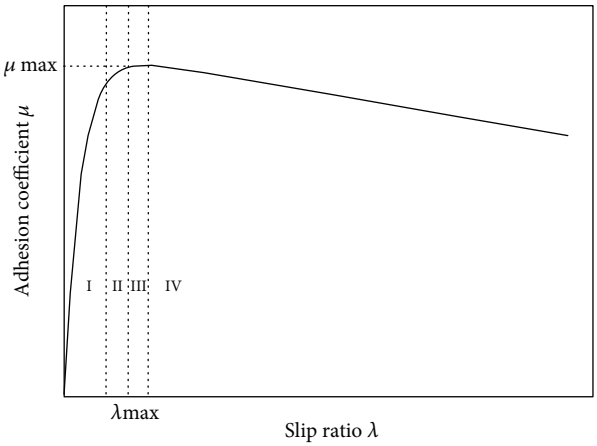


Figure 2: Relationship curve between attachment coefficient and slip ratio.

from the input that contains noise exhibit high robustness and promote the generalization capability of the AE model to input data.

Figure 3 shows that the attachment coefficient and slip ratio of the car are the input signal $x(i)$, which changes into $\tilde{x}(i)$ after noise pollution. The noise process is regarded as a random map, as shown below.

$$\tilde{x}(i) \sim qD\left(\frac{\tilde{x}(i)}{x(i)}\right), \tag{4}$$

where $qD$ is the additive noise function. SDAE conducts reduction coding on a feature set $\tilde{x}(i)$ as follows:

$$\tilde{y}(i) = f_p(\mathbf{W} \cdot \tilde{x}(i) + \mathbf{b}_1), \tag{5}$$

where $\mathbf{W}$ is the weight matrix of m × n feature, $\mathbf{b}_1$ is the encoding bias vector, and $f_p$ is the activation function.

In [21], a PReLU activation function is produced and the selection values of learning parameters are obtained. The activation function converges rapidly and the training error is small.

$$f_p = \max(0, \tilde{x}_i) + k \min(0, \tilde{x}_i), \tag{6}$$

where $k$ is the learning parameter.

SDAE is encoded to $\tilde{y} \in \mathrm{R}^m$. The reconstruction of original feature set $x(i)$ is achieved as follows:

$$\tilde{z}(i) = f_q\left(\mathrm{U}^{\mathrm{T}}\tilde{y}(\mathrm{i}) + \mathbf{b}_2\right), \quad f_q = \frac{1 - e^{-x}}{1 + e^{-x}}, \tag{7}$$

where $U \in \mathrm{R}^{m \times n}$ is the decoding matrix and $\mathbf{b}_2$ is the decoding bias vector.

The final loss function is obtained by the difference between the lost function $\tilde{z}(i)$ and the original input $x(i)$.

$$\mathrm{loss} = -\frac{1}{n}\sum_{m=1}^{n}\sum_{k=1}^{d}\left[\mathrm{x}_k^{(m)} \log\left(\tilde{z}_k^{(m)}\right) + \left(1 - x_k^{(m)}\right) \log\left(1 - \tilde{z}_k^{(m)}\right)\right] + \alpha\sum_{i=1}^{n_k} KL\frac{\rho}{\tilde{\rho}_j} + \frac{\lambda}{2}\|w\|^2, \tag{8}$$

where $d$ refers to the total number of samples, $\lambda$ is the attenuation coefficient of weight, $\|w\|$ is the item weight decay, $\alpha$ is the weight coefficient of punishment, $n_k$ represents the number of hidden layer nodes in the $k$ synergy sparse encoder, $\rho$ is the expected average excitation response of $\tilde{y}(i)$, and $\tilde{\rho}_j$ is the average incentive value in $j$ hidden units. This optimization problem is solved by using minibatch stochastic gradient descent (MSGD) algorithm, and $n$ in (8) denotes the size of the minibatch. $\mathrm{KL}(\rho/\tilde{\rho}_j)$ is the sparse penalty term. The calculation of relative entropy is expressed as follows [22]:

$$\mathrm{KL}\frac{\rho}{\tilde{\rho}_j} = \rho \log\frac{\rho}{\tilde{\rho}_j} + (1 - \rho)\log\frac{1 - \rho}{1 - \tilde{\rho}_j}, \quad \tilde{\rho}_j = \frac{1}{M}\sum_{i=1}^{M} f_{k,j}\left(\bar{x}_i^k\right). \tag{9}$$

After the KL variance achieves the sparse constraint, the initial features can be obtained without a redundant complete deep abstract set when $\rho$ is small. The gradient descent method is used to solve the optimization of the structure of the network parameters.

*3.2. SDAE.* SDAE extends the traditional SAE, but SDAE and SAE significantly differ in the retention of the original input information. The refractor decoding operation is added to the noise of the original input code. SDAE achieves the forecast to the original data from the loss of data. SDAE is a neural network composed of multilayers of noise from the encoders. In the coding part, the first coding layer is the second coding input. If $M$ hidden layers of laminated noise reduction exist from the coding network,

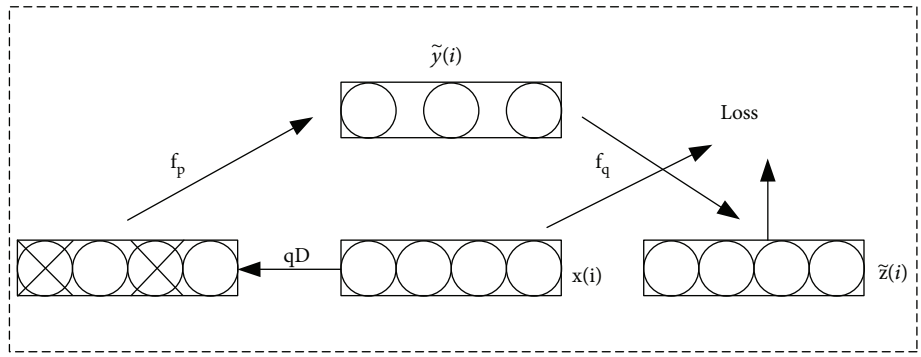


Figure 3: Weight learning.

then the $n$ layer encoder activation function can be expressed as follows:

$$\tilde{y}^{(n+1)} = f_p\left(w^{(n+1)}\tilde{y}^{(n)} + b^{(n+1)}\right), \quad n = 0, \ldots, M-1,$$
$$\tilde{y}^{(0)} = x, \tag{10}$$

where $x$ is the original data and $\tilde{y}^{(m)}$ is the car adhesion state feature selected in the $M$ coding layer. The first coding layer is regarded as the input of the second coding layer during decoding. Thus, the decoding function in $n$ layer decoder is expressed as follows:

$$\tilde{z}^{(n+1)} = f_q\left(w^{(m-n)T}z^{(n)} + b_2{}^{(n+1)}\right), \quad n = 0, \ldots, \mathrm{M}-1. \tag{11}$$

The last coding layer $\tilde{y}^{(\mathrm{m})}$ output is regarded as the input $\tilde{z}^{(0)}$ of the first decoding layer. The output $\tilde{z}^{m}$ of the decoding layer is the reconstruction of the original input data.

*3.3. Additional Classification of SVM Algorithms.* Choosing the use of a softmax classifier or SVM-based $k$ independent binary classifiers depends on whether mutex is between categories. The car adhesion conditions are normal, failure symptoms, minor faults, and the abovementioned four states. These categories are not mutually exclusive. For the failure symptom zone, a part turns into a normal state and another part becomes a small fault with the car running using an SVM classifier.

SVM is a binary classifier. A multiple classifier must be constructed to achieve the adhesion state identification for cars. In this study, a one-to-one method is used to construct a multivariate classifier. The basic idea of this method is to establish $k$ $(k-1)/2$ SVM on the basis of a large number of $k$ class problems. When classifying an unknown sample, the most votes for the last category is the category of unknown samples [23]. The algorithm is expressed as follows:

If the training data sample belongs to $k$ class and $l$ class, then binary classifiers can be converted into multiple classifiers [24].

$$\min \frac{1}{2}\left(w^{kl}\right)^T \cdot \left(w^{kl}\right) + C\sum_{i=1}^{N}\left(\xi^{kl}\right)_i \quad \xi_i \geq 0. \tag{12}$$

If $\left[\left(\mathrm{w}^{kl}\right)^T w^{kl}\right] + b^{kl} \geq 1 - \xi_i^{kl}$, then $x_i$ belongs to $k$ class. If $\left[\left(\mathrm{w}^{kl}\right)^T w^{kl}\right] + b^{kl} \leq -1 + \xi_i^{kl}$, then $x_i$ belongs to 1 class, in which slack variable $\xi_i \geq 0$; $b$ is the classification threshold, in which $w = [w_1, w_2, \cdots w^N]^T$ is the linear weight value that connects the feature space to the output space.

The kernel function used by the SVM in this study possesses an increased Gaussian radial basis kernel function.

$$K(x, x_i) = \exp\left(-\frac{\|x - x_i\|^2}{\left(2\delta^2\right)}\right), \quad \delta > 0, \tag{13}$$

where $K$ is the kernel function and $\delta$ is the kernel parameter.

*3.4. SDAE Combined with SVM.* Figure 4 shows the model of SDAE combined with SVM (SDAE-SVM). SDAE-SVM structure includes the encoding part of SDAE for feature extraction and SVM for classification.

The process of the SDAE-SVM model for identifying the car adhesion states is as follows:

(1) Parameter network weight $W$, bias $b$, and noise coefficient $qD$ are randomly initialized

(2) Input data are selected from the adhesion state set. The adhesion state set is composed of vehicle slip rate $\lambda$ and adhesion coefficient $\mu$

(3) The first layer of SDAE includes the first encoding layer and the last decoding layer. The network weights $W_1$ and bias $b_1$ are obtained. The first decoded layer obtains the adhesion status characteristic value $\tilde{y}_1$

(4) $\tilde{y}_k$ is used as the input data of the $(n+1)$th encoding layer. The $n+1$ layer of SDAE is trained to obtain

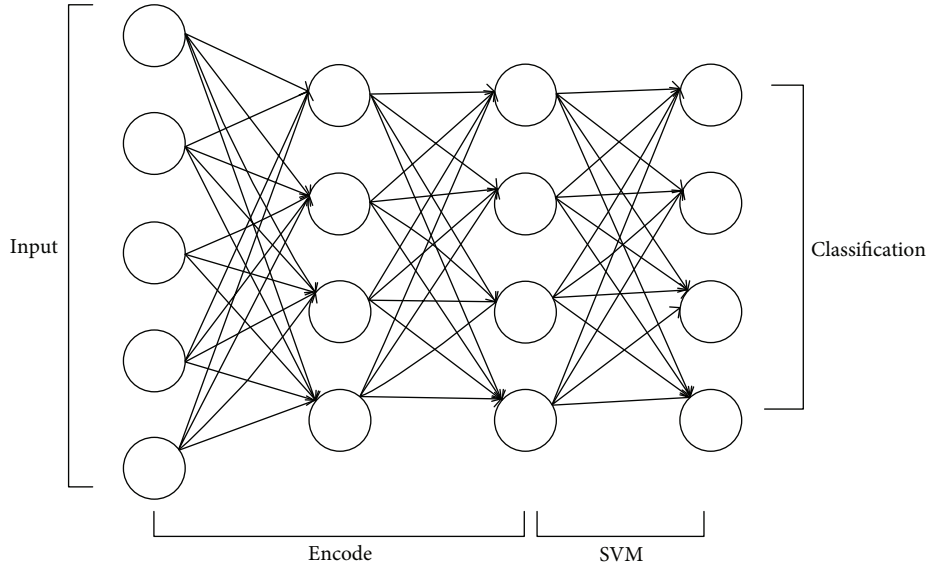


Figure 4: SDAE-SVM model.

network weights $W_{n+1}$ and bias $b_{n+1}$, and the $n+1$ layer is decoded to obtain the adhesion status characteristic value $\tilde{y}_{n+1}$. $n$ is the hidden layer

(5) Minibatch stochastic gradient descent (MSGD) algorithm is used to backpropagate the error inside the network

(6) SVM classification is used to achieve accuracy

## 4. Result Contrast and Analysis

In testing the validity of the SDAE-SVM model in feature extraction and recognition of car adhesion state, the training sample data for the training of network model must be obtained and SDAE-SVM must identify the test sets.

The experimental data are the actual sampling data. The multiengineering field, which records the adhesion state data of the vehicle skidding or idling, is used to obtain sufficient number of samples. Cars are traveling on different pavement conditions (dry asphalt, wet asphalt, dry cement, dry cobblestone, wet cobblestone, snow, and ice), thereby obtaining the adhesion state set. Speed sensors are used to collect the wheel speed $\omega$. The vehicle speed $V$ adopts the average of four wheel speeds. The slip ratio of the car can be obtained by the formula (2). The signals collected by the sensor are separated, amplified, filtered, and reshaped. The pulse signal is inputted into the computer through a data acquisition card. After the vehicle adhesion status data set under different conditions is obtained, we normalized the data in the range between 0 and 1. Three collections of adhesion status data, including 300, 1500, and 3000 sets of adhesion state data, are conducted, and the ratio of the training set sample data to the test set sample data in the attachment status data set is 1 : 1. During training, the training set is used to learn the weights and biases of each neuron. The testing set is used to produce the final classification results.

This study aims to train samples by constructing a two-layer stacking noise reduction self-coding network model, in which the number of hidden layer units in the first layer is 100 and that in the second layer is 50. During layer-by-layer training, the number of iterative trainings for each layer of the network is 100, and the learning rate is 0.01.

The experiment is conducted on the MATLAB 2010a software platform. LIBSVM, which was developed by Chang and Lin [25], is employed in the current study.

The effect of the number of nodes in the hidden layer on the accuracy of the classification on 300 data sets is shown in Figure 5.

Figure 5 shows that, when the number of hidden layer nodes is 100, the classification accuracy of SDAE-SVM is the highest. When the number of hidden layer nodes is too small, SDAE-SVM cannot fully learn the characteristics of the data. On the contrary, when the number of hidden layer nodes is too large, the learning time of SDAE-SVM significantly increases and overfitting problem occurs.

Classification accuracy is obtained to connect different Gaussian noises in testing three types of data sets, as shown in Figure 6 and Table 2.

Table 2 shows that the classification accuracy of SDAE-SVM is the highest when the added Gaussian noise is 0.5. As the noise increases, the classification accuracy of SDAE-SVM decreases slightly. A reasonable degree of denoising pretraining significantly improves the classification accuracy of the model. The use of severely damaged training data will reduce the learning capability of the model, thereby resulting in reduced classification accuracy.

Additive Gaussian noise is a very common noise model and is preferred for real-valued inputs. The salt-and-pepper and random noises will also be considered. The higher the data and the sample, the higher the accuracy of the classification. A sample set of 3000 data sets is used to study the effect of different types of noises on the classification accuracy. The results are shown in Figure 7 and Table 3.

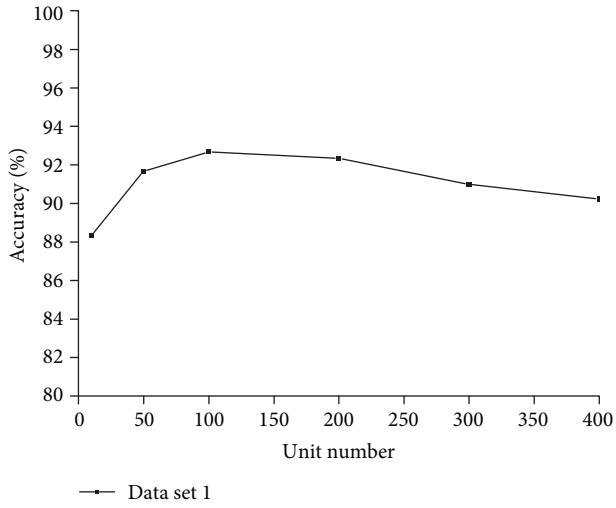


Figure 5: Relationship between the number of hidden layer nodes and classification accuracy.

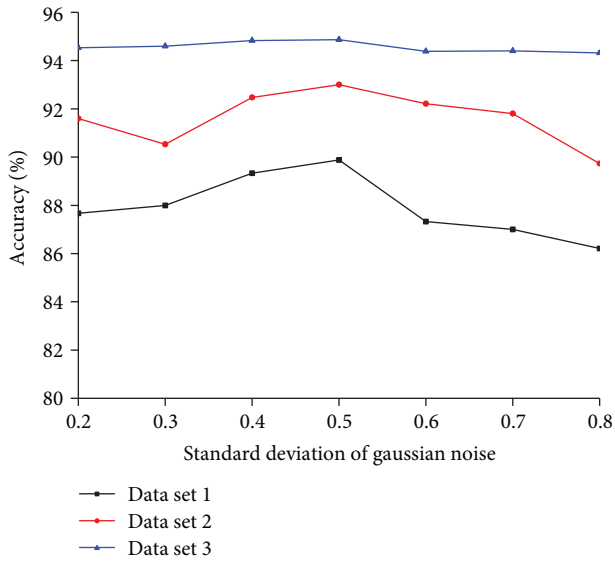


Figure 6: Effect of the standard deviation of Gaussian noise on classification accuracy.

Table 2: Effect of the standard deviation of Gaussian noise on classification accuracy (OA%).

| Sample set | 0.2 | 0.3 | 0.4 | 0.5 | 0.6 | 0.7 | 0.8 |
|---|---|---|---|---|---|---|---|
| 300 | 87.67 | 88.00 | 89.33 | 92.00 | 87.33 | 89.00 | 86.21 |
| 1500 | 91.60 | 90.53 | 92.47 | 93.00 | 92.21 | 91.80 | 89.73 |
| 3000 | 94.53 | 94.60 | 94.83 | 94.87 | 94.38 | 94.40 | 94.32 |

Denoising is a process that recovers the values of corrupted elements. Table 3 shows that the classification accuracy of SDAE-SVM is the highest when the added noise is Gaussian noise. All types of noise distribution models exhibit a few limitations. The Gaussian noise model achieves the highest accuracy rate of only 94.87%.

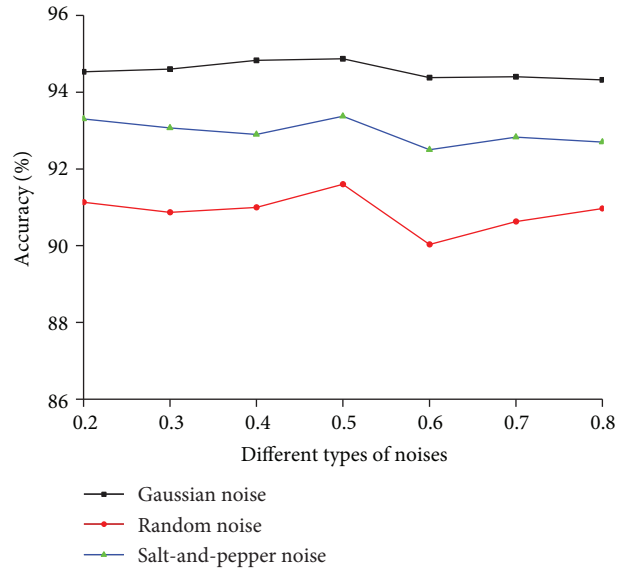


Figure 7: Effect of different types of noises on classification accuracy.

Genetic algorithm combined with SVM (GA-SVM) and extreme learning machine (ELM) [26] are used to classify the car adhesion state in verifying the classification effect of the proposed SDAE-SVM, as shown in Figure 8 and Table 4.

Table 4 shows that ELM does not obtain a high accuracy for adhesion state identification and fluctuates significantly. SDAE-SVM presents the highest accuracy in adhesion state recognition. The classification accuracy of SDAE-SVM increases gradually with the increase in data sets. This performance shows the superiority of the method in processing large data.

Table 5 shows that ELM classification consumes the shortest time. SDAE-SVM classification consumes a slightly longer time than that of ELM. GA-SVM consumes the longest time. As the sample set increases, the model consumes much time. Table 6 shows the classification accuracy using SDAE-SVM with PReLU and sigmoid functions. SDAE-SVM with PReLU function outperforms SDAE-SVM with sigmoid function on three sample sets.

## 5. Conclusion

This study aims to address feature extraction and recognition of adhesion state and proposes an identification method that combines SDAE with SVM. The effectiveness of the proposed method is validated by computer simulation. The conclusions are elaborated as follows:

(1) The adhesion state is divided into four categories, thereby providing new ideas for early risk warning of ADAS

(2) SDAE can restore the original signal subject to considerable noise. The accuracy of adhesion state feature extraction enhances the robustness of the model

Table 3: Effect of different types of noises on classification accuracy (OA%).

| Sample set 3000 | 0.2 | 0.3 | 0.4 | 0.5 | 0.6 | 0.7 | 0.8 |
|---|---|---|---|---|---|---|---|
| Gaussian noise | 94.53 | 94.60 | 94.83 | 94.87 | 94.38 | 94.40 | 94.32 |
| Random noise | 91.13 | 90.87 | 91.00 | 91.60 | 90.03 | 90.63 | 90.97 |
| Salt-and-pepper noise | 93.30 | 93.07 | 92.90 | 93.37 | 92.50 | 92.83 | 92.70 |

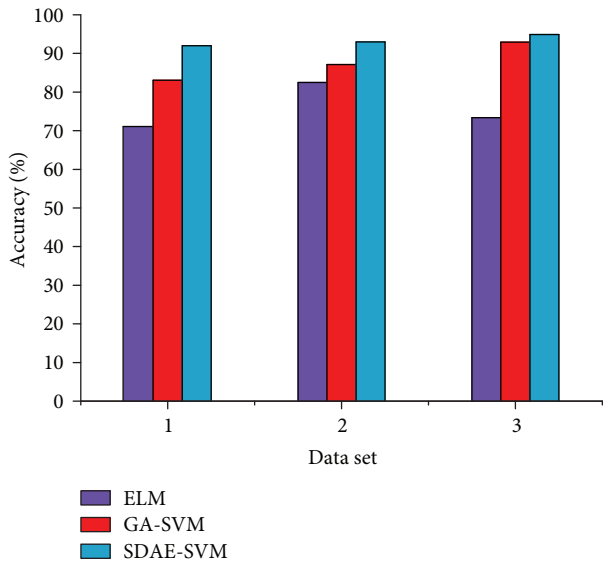


Figure 8: Comparison among the classification accuracies of SDAE-SVM, GA-SVM, and ELM.

Table 4: Comparison among the classification accuracies of SDAE-SVM, GA-SVM, and ELM (OA%).

| Sample set | ELM | GA-SVM | SDAE-SVM |
|---|---|---|---|
| 300 | 70.9 | 83.06 | 92.63 |
| 1500 | 82.5 | 87.13 | 93.00 |
| 3000 | 73.4 | 92.91 | 94.87 |

Table 5: Comparison among the classification times (in seconds) consumed by SDAE-SVM, GA-SVM, and ELM.

| Sample set | ELM | GA-SVM | SDAE-SVM |
|---|---|---|---|
| 300 | 0.08 | 17.32 | 0.18 |
| 1500 | 0.12 | 45.13 | 0.20 |
| 3000 | 0.21 | 215.04 | 0.41 |

Table 6: Classification accuracy using SDAE-SVM with PReLU and sigmoid functions (OA%).

| Sample set | PReLU | Sigmoid |
|---|---|---|
| 300 | 92.00 | 90.24 |
| 1500 | 93.00 | 91.05 |
| 3000 | 94.87 | 93.48 |

(3) The classification accuracy of SDAE-SVM is higher than that of ELM and GA-SVM, and its adhesion state identification performs well

## Conflicts of Interest

The authors declare that there is no conflict of interests.

## Acknowledgments

This study was supported by the Natural Science Foundation of China (nos. 61773159, 61473117), Hunan Provincial Natural Science Foundation of China (nos. 2018JJ2093, 2017JJ4031), Key Laboratory for Electric Drive Control and Intelligent Equipment of Hunan Province (no. 2016TP1018).

## References

[1] M. Alam, J. Ferreira, and J. Fonseca, "Introduction to intelligent transportation systems," in *Intelligent Transportation Systems*, pp. 1–17, Springer, 2016.

[2] J. Xu, P. Wang, Y. Yao, S. Liu, and G. Zhang, "3D multi-directional sensor with pyramid mirror and structured light," *Optics and Lasers in Engineering*, vol. 93, pp. 156–163, 2017.

[3] J. Xu, B. Gao, C. Liu, P. Wang, and S. Gao, "An omnidirectional 3D sensor with line laser scanning," *Optics and Lasers in Engineering*, vol. 84, pp. 96–104, 2016.

[4] Y. Li, Y. Qiao, and Y. Ruichek, "Multiframe-based high dynamic range monocular vision system for advanced driver assistance systems," *IEEE Sensors Journal*, vol. 15, no. 10, pp. 5433–5441, 2015.

[5] J. H. Yoon, S. Eben Li, and C. Ahn, "Estimation of vehicle sideslip angle and tire-road friction coefficient based on magnetometer with GPS," *International Journal of Automotive Technology*, vol. 17, no. 3, pp. 427–435, 2016.

[6] G. Erdogan, L. Alexander, and R. Rajamani, "Estimation of tire-road friction coefficient using a novel wireless piezoelectric tire sensor," *IEEE Sensors Journal*, vol. 11, no. 2, pp. 267–279, 2011.

[7] K. S. Han, E. Lee, and S. Choi, "Estimation of the maximum lateral tire-road friction coefficient using the 6-DoF sensor," in *2015 15th International Conference on Control, Automation and Systems (ICCAS)*, pp. 1734–1738, Busan, Republic of Korea, October 2015.

[8] D. M. Bevly, J. C. Gerdes, C. Wilson, and G. Zhang, "The use of GPS based velocity measurements for improved vehicle state estimation," in *Proceedings of the 2000 American Control Conference. ACC (IEEE Cat. No.00CH36334)*, pp. 2538–2542, Chicago, IL, USA, June 2000.

[9] K. Enisz, I. Szalay, G. Kohlrusz, and D. Fodor, "Tyre–road friction coefficient estimation based on the discrete-time extended Kalman filter," *Proceedings of the Institution of Mechanical*

*Engineers, Part D: Journal of Automobile Engineering*, vol. 229, no. 9, pp. 1158–1168, 2015.

[10] G. Xu, K. Xu, C. Zheng, and T. Zahid, "Optimal operation point detection based on force transmitting behavior for wheel slip prevention of electric vehicles," *IEEE Transactions on Intelligent Transportation Systems*, vol. 17, no. 2, pp. 481–490, 2016.

[11] L. Li, K. Yang, G. Jia, X. Ran, J. Song, and Z. Q. Han, "Comprehensive tire–road friction coefficient estimation based on signal fusion method under complex maneuvering operations," *Mechanical Systems and Signal Processing*, vol. 56-57, no. 56, pp. 259–276, 2015.

[12] J. Schmidhuber, "Deep learning in neural networks: an overview," *Neural Networks*, vol. 61, pp. 85–117, 2015.

[13] C. Zhang, J. Song, Z. Pei, and J. Jiang, "An imbalanced data classification algorithm of de-noising auto-encoder neural network based on SMOTE," *MATEC Web of Conferences*, vol. 56, 2016.

[14] Y. Ueda, L. Wang, A. Kai, X. Xiao, E. S. Chng, and H. Li, "Single-channel dereverberation for distant-talking speech recognition by combining denoising autoencoder and temporal structure normalization," *Journal of Signal Processing Systems*, vol. 82, no. 2, pp. 151–161, 2016.

[15] J. Li, Z. Struzik, L. Zhang, and A. Cichocki, "Feature learning from incomplete EEG with denoising autoencoder," *Neurocomputing*, vol. 165, pp. 23–31, 2015.

[16] R. Xia, J. Deng, B. Schuller, and Y. Liu, "Modeling gender information for emotion recognition using denoising autoencoder," in *2014 IEEE International Conference on Acoustics, Speech and Signal Processing (ICASSP)*, pp. 990–994, Florence, Italy, 2014, IEEE.

[17] G. Yin, S. Wang, and X. Jin, "Optimal slip ratio based fuzzy control of acceleration slip regulation for four-wheel independent driving electric vehicles," *Mathematical Problems in Engineering*, vol. 2013, Article ID 410864, 7 pages, 2013.

[18] Y. Wang, Y. Jia, X. Li, and N. Xi, "Dynamics modeling of a mobile manipulator for wheel slip avoidance," in *2011 IEEE International Conference on Robotics and Biomimetics*, pp. 1621–1626, Karon Beach, Phuket, Thailand, 2011.

[19] X. Xia, L. Xiong, K. Sun, and Z. P. Yu, "Estimation of maximum road friction coefficient based on Lyapunov method," *International Journal of Automotive Technology*, vol. 17, no. 6, pp. 991–1002, 2016.

[20] L. Li, D. Wen, N. N. Zheng, and L. C. Shen, "Cognitive cars: a new frontier for ADAS research," *IEEE Transactions on Intelligent Transportation Systems*, vol. 13, no. 1, pp. 395–407, 2012.

[21] K. He, X. Zhang, S. Ren, and J. Sun, "Delving deep into rectifiers: surpassing human-level performance on imagenet classification," in *2015 IEEE International Conference on Computer Vision (ICCV)*, pp. 1026–1034, Santiago, Chile, 2015.

[22] C. Xing, L. Ma, and X. Yang, "Stacked Denoise autoencoder based feature extraction and classification for hyperspectral images," *Journal of Sensors*, vol. 2016, Article ID 3632943, 10 pages, 2016.

[23] Z. X. Yang, Y. H. Shao, and X. S. Zhang, "Multiple birth support vector machine for multi-class classification," *Neural Computing and Applications*, vol. 22, Supplement 1, pp. 153–161, 2013.

[24] C. P. Lee and C. J. Lin, "A study on L2-loss (squared hinge-loss) multiclass SVM," *Neural computation*, vol. 25, no. 5, pp. 1302–1323, 2013.

[25] C. C. Chang and C. J. Lin, "LIBSVM: a library for support vector machines," *ACM Transactions on Intelligent Systems and Technology*, vol. 2, no. 3, pp. 1–27, 2011.

[26] Y. Yu, Z. Long, N. Xi, Y. Jia, and C. Ding, "Local path planning based on ridge regression extreme learning machines for an outdoor robot," in *2015 IEEE International Conference on Robotics and Biomimetics (ROBIO)*, pp. 745–750, Zhuhai, China, December 2016.